XLIII CILAMCE
21–25, November, 2022
FOZ DO IGUAÇU – PR – BRAZIL

GFEM modeling bending of Functionally Graded Material (FGM) plates

Bruno P. Santos[1], Paulo de Tarso R. Mendonça[1]

[1]*Dept. of Mechanical Engineering, Federal University of Santa Catarina (UFSC)*
Centro Tecnológico, Campus Universitário, Trindade, 88040-900, Santa Catarina, Brazil
bruno.pe.santos1@gmail.com, mendonca@grante.ufsc.br

Abstract. This paper presents a Generalized Finite Element Method (GFEM) formulation for mechanical analysis of Functionally Graded Material (FGM) plates acting both under mechanical loads and under the effect of high gradient thermal fields. It describes the development, implementation and validation of said formulation, based on a composite plate model ruled by Reissner-Mindlin's first-order shear theory. The calculation of temperature field along the structure's thickness is made by solving the stead-state heat conduction problem through Finite Difference Method, considering given the boundary conditions on both faces of the plate and thermal conductivities of the base materials. Elasticity moduli and thermal conductivities' temperature-dependence is considered. Thickness-wise numerical integration procedures are used to compute both the stiffness matrices of the plate and the thermal portions of nodal force vectors. A C^k continuous GFEM model with three-noded triangular shaped elements is considered and a linear strain-displacement relationship is adopted. Shepard Partitions of unit with smooth approximation functions are used and enriched by linearly independent polynomials. Solutions are obtained through Newton-Raphson method.

Keywords: Functionally graded material, Generalized finite element method, Reissner-Mindlin's model

1 Introduction

Due to the increasing usage of FGM in the construction of space shuttles and other structures designed to operate in environments with harsh thermal conditions, it is important to further develop analysis models capable of representing the coupling of mechanical and thermal effects in this kind of composite. Being a relatively new kind of material, initially developed in 1987 by the Science and Technology Agency, of Japan [1], much research has been done in the area, namely by authors such as Reddy [2] and Park and Kim [3], but there are still many topics that need to be researched and understood.

Parallel to this, in recent years, GFEM has risen as a valuable alternative to conventional FEM and meshless methods in the solution of boundary value problems, having less dependency on mesh geometry than conventional FEM and lower computational cost than the main meshless methods as well as easier implementation of Dirichlet boundary conditions. An important advance in this area was made by de Barcellos et al. [4], who developed a C^k continuous formulation of the method. Given that GFEM may be a valuable tool in the analysis of complex materials, this paper aims to initiate and instigate the development GFEM models for FGM plates.

2 Theoretical Formulation

2.1 FGM Properties

As proposed by Reddy [5], eq. 1 represents material properties' gradation through the thickness of the plate, being $V_c(z)$ the volume fraction of ceramic material at a certain coordinate z, P_c and P_m the

properties of the metallic and ceramic materials and n the FGM's distribution parameter.

$$P(z) = (P_c - P_m)V_c + P_m,$$
$$V_c(z) = \left(\frac{1}{2} + \frac{z}{H}\right)^n \qquad n \geq 0, \tag{1}$$

For the purposes of this study, ν and α are considered to be constant for both materials, while E and k are considered to be temperature dependent, following eq. 2 [3].

$$P_m(T) \text{ (or } P_c(T)) \ = P_o(P_{-1}T^{-1} + 1 + P_1T + P_2T^3 + P_3T^3) \tag{2}$$

It's important to observe that, even though the plate is a composite structure, each point of it behaves isotropically. Figure 1 represents the FGM's geometry and composition.

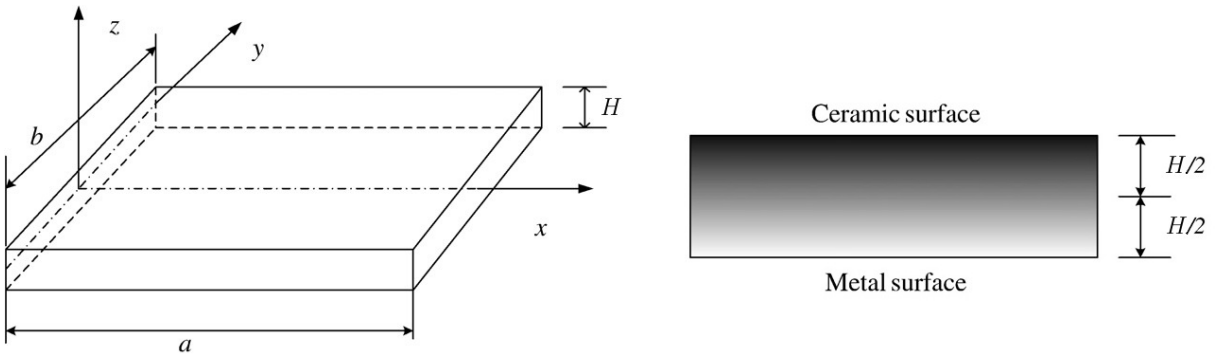

Figure 1. FGM plate's geometry and coordinate system. Source: Lee et al. [6], adapted

2.2 Mechanical behavior

Reissner-Mindlin's plate theory is one of the main First-order Shear Deformation Theories (FSTD), and may be represented by the following set of equations [7].

$$\begin{aligned} u(x,y,z) &= u^o(x,y) + z\phi_x(x,y), \\ v(x,y,z) &= v^o(x,y) + z\phi_y(x,y), \\ w(x,y,z) &= w(x,y) \end{aligned} \tag{3}$$

where u, v and w are the coordinates of a point in the deformed configuration, index $(\ )^o$ represents the position of the plate's reference plane and ϕ_x e ϕ_y are cross-section rotations around axis x and y.

$$\phi_x = \frac{\partial u}{\partial z}, \qquad \phi_y = \frac{\partial v}{\partial z} \tag{4}$$

Bending behavior of a Mindlin plate under mechanical loads can then be described by the constitutive equations:

$$\left\{ \begin{array}{c} \mathbf{N} \\ \mathbf{M} \end{array} \right\} = \left[\begin{array}{cc} \mathbf{A} & \mathbf{B} \\ \mathbf{B} & \mathbf{D} \end{array} \right] \left\{ \begin{array}{c} \boldsymbol{\varepsilon}^o \\ \boldsymbol{\kappa} \end{array} \right\}, \tag{5}$$
$$\mathbf{Q}_t = \mathbf{E}\boldsymbol{\gamma}_c,$$

where

$$\mathbf{A} = \int_{-H/2}^{H/2} \mathbf{Q}\ dz, \qquad \mathbf{B} = \int_{-H/2}^{H/2} z\mathbf{Q}\ dz, \qquad \mathbf{D} = \int_{-H/2}^{H/2} z^2\mathbf{Q}\ dz \tag{6}$$

and

$$\mathbf{E} = k\int_{-H/2}^{H/2} \mathbf{e}\ dz, \qquad \mathbf{e} = \left[\begin{array}{cc} C_{44}^x & C_{45}^x \\ C_{45}^x & C_{55}^x \end{array} \right] \tag{7}$$

In the analysis of laminated composite eqs. 6 and 7 and generally computed through the sum of layer-wise components. However, as FGM aren't divided in layers and their properties aren't easily

computed by analytic integration, these matrices must generally be calculated by numeric integration processes or other approximation methods. This paper uses Simpson's 3/8 rule to compute these and other through-thickness integrals, dividing the coordinate's domain into a series of sub-intervals and integrating each one by cubic polynomial approximations.

Considerations about deformations due to effect of the thermal field will be made in Section 2.4.

2.3 Temperature field distribution

The temperature field $T(z)$ is given by the solution of a one-dimensional stead state heat conduction problem, with prescribed temperatures on the boundaries and no internal heat sources. Equation 8 presents this problem [5], being $k(z,T)$ the FGM's thermal conductivity. .

$$\begin{aligned} -\frac{d}{dz}\left(k(z,T)\frac{dT}{dz}\right) &= 0 \qquad \text{in } z \in (-H/2, H/2), \\ T(-H/2) &= T_m, \\ T(H/2) &= T_c, \end{aligned} \tag{8}$$

Due to the dependency that $k(z,T)$ has on the distribution of ceramic and metallic material in the plate, an analytical solution for an arbitrary value of n is not possible. Therefore, this solution is usually obtained numerically, through methods such as the Finite Difference Method (FDM), used in this study. Furthermore, as this paper considers the effect of temperature in the conductivity $k(z,T)$, an iterative procedure had to be adopted to compute $T(z)$. The L_2-norm loss function was used to evaluate convergence.

2.4 Thermal effects in bending

Since FGM are considered to be isotropic at each coordinate z, the stress-strain relationship for the FSTD model can be expressed by eq. 9.

$$\left\{\begin{array}{c}\sigma_x\\ \sigma_y\\ \tau_{xy}\end{array}\right\} = \left[\begin{array}{ccc} Q_{11} & Q_{12} & \\ Q_{12} & Q_{22} & \\ & & Q_{66}\end{array}\right] \left\{\begin{array}{c}\varepsilon_x - \alpha\Delta T\\ \varepsilon_y - \alpha\Delta T\\ \gamma_{xy}\end{array}\right\} \quad \rightarrow \quad \boldsymbol{\sigma} = \mathbf{Q}\left(\boldsymbol{\varepsilon} - {}^{\mathcal{T}}\boldsymbol{\varepsilon}\right) \tag{9}$$

where ${}^{\mathcal{T}}\varepsilon = \alpha\Delta T\mathbf{1}$ is the strain component due to thermal dilation, and $\mathbf{1} = \{1,1,0\}^T$. Transverse shear equations aren't affected by temperature effects:

$$\left\{\begin{array}{c}\tau_{yz}\\ \tau_{xz}\end{array}\right\} = \left[\begin{array}{cc} Q_{44} & \\ & Q_{55}\end{array}\right] \left\{\begin{array}{c}\gamma_{yz}\\ \gamma_{xz}\end{array}\right\} \quad \rightarrow \quad \boldsymbol{\tau} = \mathbf{Q}^s\boldsymbol{\gamma} \tag{10}$$

Isotropic behavior determines that $Q_{11} = Q_{22} = E/(1-v^2)$, $Q_{12} = vQ_{11}$, $Q_{66} = E/2(1+v)$, and $Q_{44} = Q_{55} = E/2(1+v)$.

Given the constitutive equation described by eq. 5, it is true for FSTD that:

$$\boldsymbol{\varepsilon} = \boldsymbol{\varepsilon}^o + z\boldsymbol{\kappa} \tag{11}$$

A constitutive equation for FGM under thermomechanical effects can be obtained from the definition of in-plane and moment force resultants, described in eq. 12.

$$\mathbf{N} = \int_{-H/2}^{H/2} \boldsymbol{\sigma}\, dz \qquad \text{and} \qquad \mathbf{M} = \int_{-H/2}^{H/2} \boldsymbol{\sigma} z\, dz. \tag{12}$$

Applying eqs. 9 and 11 to the in-plane force resultant in eq. 12,

$$\mathbf{N} = \underbrace{\int_{-H/2}^{H/2} \mathbf{Q}\, dz\boldsymbol{\varepsilon}^o}_{\mathbf{A}} + \underbrace{\int_{-H/2}^{H/2} z\mathbf{Q}\, dz\boldsymbol{\kappa}}_{\mathbf{B}} - \underbrace{\int_{-H/2}^{H/2} \mathbf{Q}\, {}^{\mathcal{T}}\boldsymbol{\varepsilon}\, dz}_{{}^{\mathcal{T}}\mathbf{N}} \tag{13}$$

Similarly, for the moment force resultant:

$$\mathbf{M} = \underbrace{\int_{-H/2}^{H/2} \mathbf{Q} z \; dz \boldsymbol{\varepsilon}^o}_{\mathbf{B}} + \underbrace{\int_{-H/2}^{H/2} z^2 \mathbf{Q} \; dz \boldsymbol{\kappa}}_{\mathbf{D}} - \underbrace{\int_{-H/2}^{H/2} \mathbf{Q} \; {}^{\mathcal{T}}\boldsymbol{\varepsilon} z \; dz}_{{}^{\mathcal{T}}\mathbf{M}} \tag{14}$$

The thermal components in eqs. 14 and 13 are given by:

$${}^{\mathcal{T}}\mathbf{N} = \underbrace{\int_{-H/2}^{H/2} \mathbf{Q} \alpha \Delta T \; dz \mathbf{1}}_{{}^0\mathbf{Q}} = {}^0\mathbf{Q}\mathbf{1} \qquad \text{and} \qquad {}^{\mathcal{T}}\mathbf{M} = \underbrace{\int_{-H/2}^{H/2} \mathbf{Q} \alpha \Delta T z \; dz \mathbf{1}}_{{}^1\mathbf{Q}} = {}^1\mathbf{Q}\mathbf{1}. \tag{15}$$

Hence, the FGM plate's constitutive relation becomes:

$$\left\{ \begin{array}{c} \mathbf{N} \\ \mathbf{M} \end{array} \right\} = \left[\begin{array}{cc} \mathbf{A} & \mathbf{B} \\ \mathbf{B} & \mathbf{D} \end{array} \right] \left\{ \begin{array}{c} \boldsymbol{\varepsilon}^o \\ \boldsymbol{\kappa} \end{array} \right\} - \left\{ \begin{array}{c} {}^{\mathcal{T}}\mathbf{N} \\ {}^{\mathcal{T}}\mathbf{M} \end{array} \right\}, \quad \text{where} \quad \left\{ \begin{array}{c} {}^{\mathcal{T}}\mathbf{N} \\ {}^{\mathcal{T}}\mathbf{M} \end{array} \right\} = \left\{ \begin{array}{c} {}^0\mathbf{Q} \\ {}^1\mathbf{Q} \end{array} \right\} \mathbf{1}. \tag{16}$$

It's noticeable that this relation is formally the same used for anisotropic laminates. However, the procedure for computing the constitutive matrices $\mathbf{A}$, $\mathbf{B}$, $\mathbf{D}$, ${}^0\mathbf{Q}$ e ${}^1\mathbf{Q}$ is different and must be done via numeric integration.

2.5 GFEM applied to FGM

As presented by Mendonça [7], from the matrix equation that represents the approximated form of Principle of Virtual Work (PVW) for FSTD plates it is possible to obtain, in compact notation,

$$[\mathbf{K}_f + \mathbf{K}_c] \, \mathbf{U} = \mathbf{F} \tag{17}$$

being $\mathbf{U}$ the nodal displacement vector, $\mathbf{F}$ the nodal force vector, and $\mathbf{K}_f$ and $\mathbf{K}_c$ stiffness matrices.

Thermal deformation introduces a new force component, defined in eq. 18, which must be added to the vector representing mechanical loads in order to form the nodal force vector $\mathbf{F}$.

$${}^{\mathcal{T}}\mathbf{F} = \int_\Omega \mathbf{B}_f^T \left\{ \begin{array}{c} {}^{\mathcal{T}}\mathbf{N} \\ {}^{\mathcal{T}}\mathbf{M} \end{array} \right\} d\Omega, \tag{18}$$

Therefore, eq. 17 becomes:

$$[\mathbf{K}_f + \mathbf{K}_c] \, \mathbf{U} = \; {}^m\mathbf{F} + {}^{\mathcal{T}}\mathbf{F} \tag{19}$$

The usage of FEM shape functions as a Partition of Unit (PU) that can be enriched by a set of linearly independent functions defines GFEM. Thus, it is possible to increase their capability of representing solutions without the need of increasing complexity and number of elements. For this study, polynomial enrichment functions were used.

3 Numerical results

Two FGM problems were analyzed to validate the GFEM formulation developed and analytical solutions were used to verify numerical results. In both cases, the square plates where divided into a regular mesh of 128 triangular elements with linear shape functions, and GFEM enrichment was performed through the usage of quartic polynomial functions. The solutions were obtained by using Newton-Raphson's method.

3.1 Material properties

The materials adopted to compose the FGM plate were stainless steel and zirconia. Both materials were considered to have Poisson ratio $\nu = 0.3$ and temperature-independent thermal expansion coefficients $\alpha_m = 1.682 \times 10^{-5}$ K^{-1} and $\alpha_c = 3.013 \times 10^{-5}$ K^{-1}. Elasticity moduli and thermal conductivities were considered to behave as described by eq. 2 and their coefficients are presented at Table 1 [2].

Table 1. FGM plate's temperature-dependent material properties

Property	P_0	P_{-1}	P_1	P_2	P_3
E_m (Pa)	201.04×10^9	0	3.079×10^{-4}	-6.534×10^{-7}	0
E_c (Pa)	244.27×10^9	0	-1.371×10^{-3}	-1.214×10^{-6}	-3.681×10^{-10}
k_m (W/mK)	15.379	0	-1.264×10^{-3}	2.092×10^{-6}	-7.223×10^{-10}
k_c (W/mK)	1.7000	0	1.276×10^{-4}	6.648×10^{-8}	0

3.2 Square Mindlin FGM plate under thermal bending

A square plate with length $L = 0.5$ m, thickness $H = 0.05$ m and distribution coefficient $n = 1.0$ was considered to be simply supported over its vertices. Top and bottom temperatures were assumed as $T_c = 600$K and $T_m = 300$K and deformation was considered to originate solely from thermal dilation. Figure 2 represents material distribution over thickness and the temperature field computed with FDM.

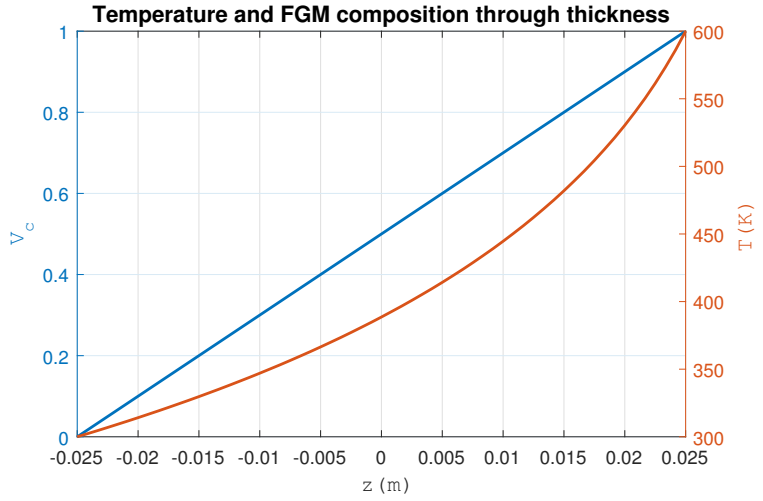

Figure 2. Volumetric fraction of ceramic $V_c(z)$ and temperature field $T(z)$ over plate's thickness

Figure 3 shows the results obtained using GFEM (due to the orthogonal symmetry of the problem, v^o and ψ_y^o possess behavior equivalent to that shown for u^o and ψ_x^o). An analytical solution was created and used as reference to calculate the errors of the numerical model.

At Table 2 the maximum value of each type of displacement in Mindlin's plate theory is presented, as well as relative errors associated to those values, maximum errors over the studied domain and Mean Squared Error of the mesh's nodes.

Table 2. Results of GFEM analysis of FGM under thermal bending

Displacement	Maximum	Error max. displ.(%)	Max. Error(%)	MSE
w^o (m)	$9.60 \cdot 10^{-3}$	0.012	0.012	$1.4 \cdot 10^{-8}$
u^o (m)	$6.92 \cdot 10^{-4}$	0.011	0.015	$7.6 \cdot 10^{-9}$
v^o (m)	$6.92 \cdot 10^{-4}$	0.010	0.015	$7.6 \cdot 10^{-9}$
ψ_x^o	0.0383	0.012	0.012	$1.3 \cdot 10^{-8}$
ψ_y^o	0.0383	0.012	0.012	$1.3 \cdot 10^{-8}$

By analyzing this data, it's possible to perceive that the GFEM model was able to accurately represent the deformed configuration of the FGM plate, producing small errors (with order of magnitude

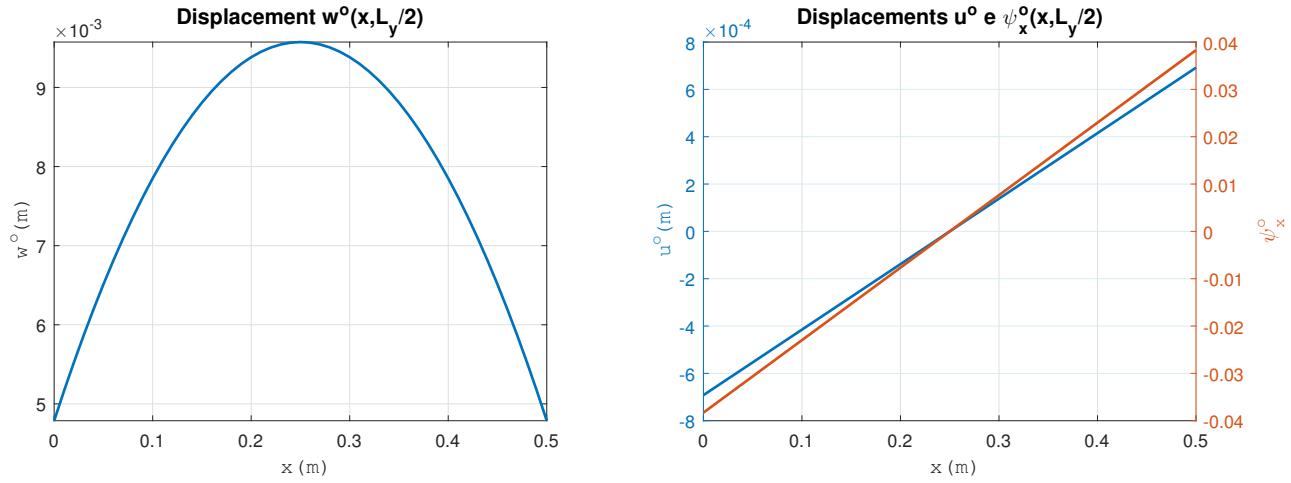

Figure 3. Displacements over x (behavior of v^o and ψ_y^o over y is similar to that of u^o and ψ_x^o, respectively)

of 0,01%).

3.3 Square thin FGM plate under mechanical bending

The second situation analyzed was that of a thin FGM plate (length $L_x = L_y = 0.5$ m and $H = 0.001$) with distribution coefficient $n = 1.0$. This plate was considered to be simply supported over its edges, $x = 0, L_x$ and $y = 0, L_y$, and submitted to transversal load as described by eq. 20, with $q_{mn} = 100$ Pa. For this case of study, there weren't considered to exist stresses related to thermal effects.

$$q(x, y) = q_{mn} \operatorname{sen} \frac{\pi x}{L_x} \operatorname{sen} \frac{\pi y}{L_y} \tag{20}$$

Because of its reduced thickness, this problem can be considered to be a Kirchoff plate, and the analytical solution with that theory described as:

$$\left\| \begin{aligned} u^o(x, y) &= U_{mn} \cos(\pi L_x^{-1} x) \operatorname{sen}(\pi L_y^{-1} y), \\ v^o(x, y) &= V_{mn} \operatorname{sen}(\pi L_x^{-1} x) \cos(\pi L_y^{-1} y), \\ w^o(x, y) &= W_{mn} \operatorname{sen}(\pi L_x^{-1} x) \operatorname{sen} \pi(L_y^{-1} y), \end{aligned} \right. \tag{21}$$

being that, after considering the assumptions made for this problem, the coefficients U_{mn}, V_{mn} and W_{mn} become $U_{mn} = V_{mn} = -1.0355 \cdot 10^{-7}$ m and $W_{mn} = 9.3557 \cdot 10^{-4}$ m.

Figure 4 shows the displacements w^o and u^o calculated with the developed formulation at the coordinate $y = L_y/2$, where their values reach their maximum. Displacement v^o behaves at $x = L_x/2$ in the same way shown for u^o.

The maximum value of each displacement and the relative errors associated to them are presented at Table 3, as well as the MSE of the model's nodes.

Table 3. Results of GFEM analysis of a thin FGM plate under sinusoidal load

Displacement	Maximum	Error max. displ.(%)	Max. Error(%)	MSE
w^o (m)	$9.356 \cdot 10^{-4}$	$1.4{\cdot}10^{-3}$	0.011	$5.0 \cdot 10^{-10}$
u^o (m)	$1.036{\cdot}10^{-7}$	$1.3{\cdot}10^{-3}$	0.056	$2.0 \cdot 10^{-8}$
v^o (m)	$1.036{\cdot}10^{-7}$	$1.2{\cdot}10^{-3}$	0.056	$1.9 \cdot 10^{-8}$

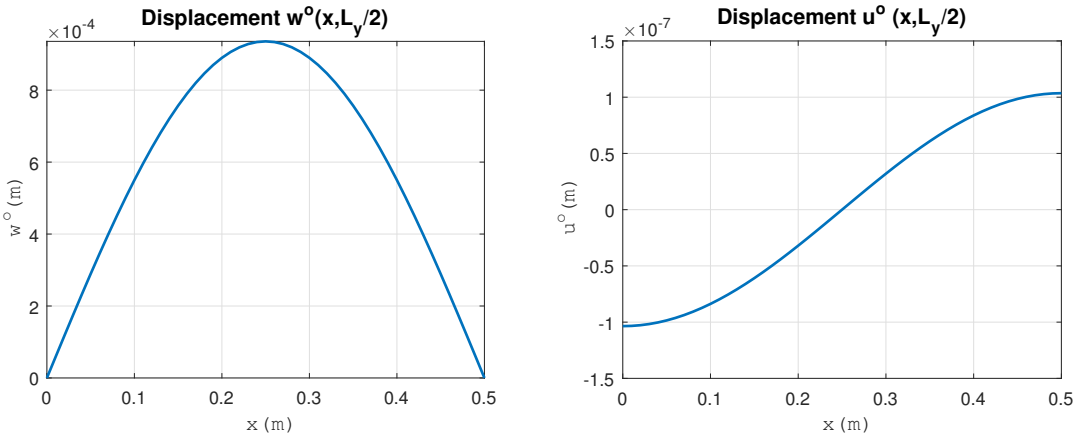

Figure 4. Displacements w^o and u^o over x (behavior of v^o over y is similar to that of u^o over x)

As with the results for the thermal problem, it's possible to see that the errors associated with the numerical solution aren't expressive, with a maximum relative error of 0.056% in a non-critical region and MSE below 10^{-7} for the studied structure.

4 Conclusions

The developed GFEM model was able to accurately represent FGM plates, both under stresses originated from harsh thermal gradients and mechanical loads. The temperature dependence of thermal conductivities was incorporated to the existing mechanical models of FGM plates and the developed theoretical and numerical advances were successfully validated through comparison with analytical solutions.

Acknowledgements. This work was supported by CNPq (Conselho Nacional de Desenvolvimento Científico e Tecnológico, Brazil).

Authorship statement. The authors hereby confirm that they are the sole liable persons responsible for the authorship of this work, and that all material that has been herein included as part of the present paper is either the property (and authorship) of the authors, or has the permission of the owners to be included here.

References

[1] M. Koizumi and M. Niino. Overview of fgm research in japan. *MRS Bulletin*, vol. 20, pp. 19–21, 1995.
[2] J. N. Reddy. Thermomechanical analysis of functionally graded cylinders and plates. *Journal of Thermal Stresses*, vol. 21, pp. 593–626, 1998.
[3] J.-S. Park and J.-H. Kim. Thermal postbuckling and vibration analyses of functionally graded plates. *Journal of Sound and Vibration*, vol. 289, pp. 77–93, 2006.
[4] de C. S. Barcellos, P. T. R. MendonÇa, and C. A. Duarte. A ck continuous generalized finite element formulation applied to laminate kirchhoff plate model. *Comput Mech*, vol. 44, pp. 377–393, 2009.
[5] J. N. Reddy. Analysis of functionally graded plates. *International Journal for Numerical Methods in Engineering*, vol. 47, pp. 663–684, 2000.
[6] Y. Lee, X. Zhao, and J. Reddy. Postbuckling analysis of functionally graded plates subject to compressive and thermal loads. *Computer Methods in Applied Mechanics and Engineering*, vol. 199, n. 25, pp. 1645–1653, 2010.
[7] P. T. R. Mendonça. *Materiais compostos e estruturas sanduíche: projeto e análise*. Editora Orsa Maggiore, Florianópolis, Brazil, 2nd edition, 2019.